Tikhomirova and Trufanov *Mechanics of Advanced Materials and Modern Processes* (2016) 2:1
DOI 10.1186/s40759-016-0008-7

Mechanics of Advanced Materials and Modern Processes
a SpringerOpen Journal

RESEARCH Open Access

Post-buckled equilibrium state of axially compressed polymeric rod in glass and rubbery transitions

Ksenia Alekseevna Tikhomirova[1*] and Nikolay Aleksandrovich Trufanov[2]

Abstract

Background: Glass and rubbery transitions under cooling and heating of polymeric materials underlie a shape memory effect, that is a material ability to save temporarily the deformed shape and restore the original one under the external influence. The present work aims to model the shape memory effect for an axially compressed polymeric rod in its post-buckled equilibrium state, which is the generalization of Euler's elastica for a glassy material case.

Methods: For modeling, we use a new type of constitutive relations describing the thermomechanical behavior of amorphous polymers over a wide temperature range. To define the model parameters for lightly-linked epoxy resin a series of experiments was conducted using the Dynamic Mechanical Analyzer.

Results: Post-buckled states of an epoxy rod equilibrium during the temperature change have been found from numerical simulation. The obtained results illustrate the shape memory effect in case of axially compressed rod buckling.

Conclusion: The thermomechanical shape-memory cycle includes the stages of deformation development and preservation and the subsequent recovery of the initial shape. According to the obtained results, maximum deflection corresponds to the first loading step at the rubbery material state, because the elastic modulus is very low. During cooling under a constant load the deformation remains constant. After unloading in glassy state the deflection decreases by a small value, because the glassy elastic modulus significantly exceeds the rubbery one. During subsequent heating the rod recovers its initial undeformed shape.

Keywords: Glass and rubbery transition, Thermomechanics, Post-buckled equilibrium state, Axial compression, Euler's elastica, Shape memory polymer, Epoxy resin

Background

Due to a high-molecular structure polymeric materials are very temperature-dependent in their mechanical properties. Glass and rubbery transitions under cooling and heating are a good illustration of such dependence. Mechanical effects occurring during glass transition, particularly for epoxy resins, are well-investigated (Liu et al. 2004, Michels et al. 2015, Shardakov et al. 1991). A large number of studies have reported on modeling these effects for the case of small deformations. Two formal groups could be derived from the studies: the models of instantaneous elastic relaxation or phase transition (Bartenev and Barteneva 1992, Bugakov 1989, Klychnikov et al. 1980) and the models based on the postulates of the non-isothermal viscous elasticity (Bolotin 1972, Il'ushin and Pobedria 1970, Moskvitin 1972). The approach used in the present study (Matveenko et al. 2012) occupies an intermediate position between these two.

Glass transition of amorphous polymers underlies a shape memory effect, that is a material ability to save temporarily the deformed shape and restore the original one under the external influence, e.g. heat. Shape memory polymers (SMP) are capable of very large recoverable strains. Such materials have been used extensively in medicine (Yakacki and Gall 2010, Yakacki et al. 2007, Sharifi et al. 2013), microelectronics and some other industrial fields (Hager et al. 2015).

* Correspondence: tikhomirova.k@icmm.ru
[1]Laboratory of Nonlinear Mechanics of Solids, Institute of Continuous Media Mechanics, Academician Korolev Street, Perm 614013, Russia
Full list of author information is available at the end of the article

Present work aims to model the shape memory effect for an axially compressed polymeric rod in its post-buckled equilibrium state. The problem of post-buckled behavior of axially compressed rods is well-documented in literature (Krylov 1931, Vol'mir 1967, Rabotnov 1988). Our study generalizes the existing analytical solutions for the case of an SMP rod thermomechanical loading.

Methods

Constitutive equations for glassy material

Glass transition is accompanied by changes of mechanical properties in transition through the region with T_{g1} and T_{g2} temperature bounds, which is connected with the molecular mobility restriction. The material comes to its glassy state at temperatures below T_{g1} and to rubbery state at temperatures above T_{g2}.

To derive the constitutive equations we use the following simplifying hypotheses (Matveenko et al. 2012):

1) the characteristic times of the external actions are much shorter than the relaxation times in the glassy state ($T < T_{g1}$, Fig. 1), so the loading process occurs more rapidly than the relaxation process;
2) the characteristic times of the external actions essentially exceed the limits of the relaxation spectrum of a highly elastic polymer ($T > T_{g2}$, Fig. 1), so all the relaxation processes finish during the loading.

With these hypotheses, beyond the limits of the glass transition interval the examined material can be considered as an elastic medium, but with different elastic moduli: E_1 —the Young's modulus for the material in the rubbery state, $E_1 + E_2$ —in the glassy state (E_2 is the difference between the glassy and rubbery moduli, for many polymeric materials $E_1 << E_2$). We assume that the polymer behavior within the glass transition interval at a decreasing temperature is specified by the growth of the mechanical rigidity due to a gradual decrease in the segmental mobility and an increase in the energy of the intermolecular interactions.

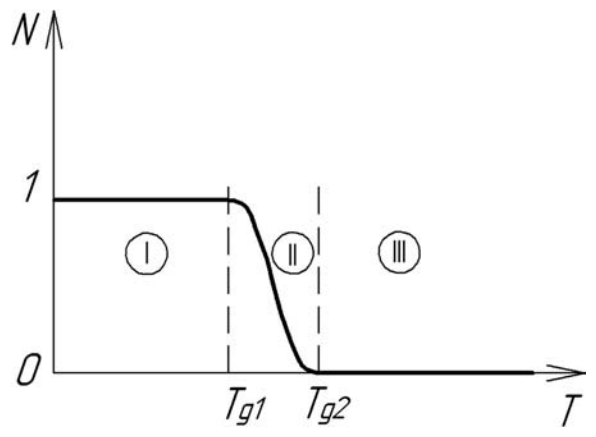

Fig. 1 Temperature-dependent conversion degree parameter $N(T)$. I—glassy region, II—transition region, III—rubbery region

To model such an effect we introduce the conversion degree parameter $N(T)$ (Fig. 1) which characterizes the degree of restriction in the segmental mobility of the polymer and changes from 0 ($T > T_{g2}$) to 1 ($T < T_{g1}$).

The hypotheses introduced above allow us to construct the constitutive relations capable of describing the behavior of SMPs over a wide range of temperatures including the transition region (Matveenko et al. 2012). In case of small strains for the uniaxial stress state they could be defined in the following way:

$$\sigma(t) = E_1(\varepsilon(t) - \varepsilon_T(t)) + E_2\int_0^t (\varepsilon(t) - \varepsilon^*(\tau))dN(\tau) - E_2\int_0^t (\varepsilon_T(t) - \varepsilon_T{}^*(\tau))dN(\tau), \quad (1)$$

where σ is the axial stress, t —the current time, ε and ε_T—the full and temperature strains, ε^* and ε_T^*—the full and temperature strains at $t = \tau^*$; τ^* is the corresponding time under the cooling conditions when $N(\tau^*) = N(\tau)$. The values of ε^* and ε_T^* are stored or frozen at the stage of vitrification and remain unchanged during the inverse transition from the glassy to rubbery state. During cooling the increase of $N(T)$ and the concurrent rigidity increase within the transition region correspond to the growth of intermolecular interaction bonds. We assume every newly formed bond to deform concurrently with the rest of the material, which is reflected in the difference form of the integrands in (1). Thus, the physical relations (1) imply that the temperature-deformation history should be reckoned from the temperature T_h (higher than T_{g2}), at which the polymer is in the equilibrium rubbery state.

Constitutive equations (1) enable us to describe the developing residual stresses and frozen strains under cooling and, correspondingly, the shape memory effect. Physically, the initiation of frozen strains is concerned with the rapidly developing relaxation processes under loading in the rubbery state (according to the hypothesis 2), which result in deformations corresponding to the elastic modulus E_1. After the vitrification due to cooling and subsequent unloading, only a small part of the total strain corresponding to the elastic modulus $E_1 + E_2$ recovers. The other, bigger part of the total strain remains frozen, since the characteristic relaxation times in the glassy state significantly exceed the limits required for the total strain recovery (hypothesis 1).

Numerical modeling

In this section, we specify some numerical aspects of the model based on the constitutive equations (1). The Laplace distribution is used to describe the conversion degree parameter $N(T)$ (Matveenko et al. 2012, Bronshtein and Semendjaiev 1986):

$$N = \begin{cases} 1 - 0,5 \exp\left(\dfrac{T - T_g}{\gamma_L}\right), & T < T_g \\ 0,5 \exp\left(-\dfrac{T - T_g}{\gamma_L}\right), & T \geq T_g \end{cases} \quad (2)$$

where γ_L is the width-like parameter for the transition region, and T_g is the parameter specifying the transition temperature.

The temperature strain included in (1) could be expressed as

$$\varepsilon_T = \alpha \Delta T. \quad (3)$$

Here ΔT is the temperature variation; and α —the linear temperature expansion coefficient (LTEC) defined as

$$\alpha = \begin{cases} \alpha_1, T > T_{g\alpha}, \\ \alpha_2, T \leq T_{g\alpha}, \end{cases} \quad (4)$$

where $T_{g\alpha}$ is the mean temperature of the transition region, α_1 and α_2 —the LTEC for the rubbery and glassy material states respectively.

Thus, the numerical model defined through the relations (1)–(4) includes seven independent parameters: $E_1, E_2, \alpha_1, \alpha_2, \gamma L, T_g$ and $T_{g\alpha}$.

Experiments

The material considered in this work is the lightly-linked epoxy resin of special composition. In order to identify the material parameters included into the relations (1)–(4) a series of experiments was conducted using a Dynamic Mechanical Analyzer DMA Q800 V20.24 Build 43. Cylindrical specimens were 5.8 mm in diameter and 7.8 mm tall. The specimens were heated under a heat rate 1.25°C/min and a constant compression load 0.25 N. The results obtained are shown in Fig. 2.

It has been established from the experimental data that the variation of the heat rate results in the thermomechanical curve shifting along the temperature axis. In this work we do not consider the heat rate influence on the thermomechanical material behavior and take the rate value as a constant.

A simple compression test at room temperature under the small strain level has also been conducted, and the value of glassy elastic modulus $E_1 + E_2 = 0,77$ GPa was obtained.

Identification of model parameters

Based on the experimental data obtained in the previous section, the parameters of the numerical model were defined.

The value of $T_{g\alpha}$ related to the inflection point of the thermomechanical curve in the middle of the transition region is taken 80°C. The glass transition bounds were taken as $T_{g1} = 55\,^{\circ}\mathrm{C}$ and $T_{g2} = 105\,^{\circ}\mathrm{C}$ according to the shape of the thermomechanical curve (Fig. 2).

The parameters $E_1, \alpha_1, \alpha_2, \gamma L$ and T_g were defined from the better concordance between the experimental and

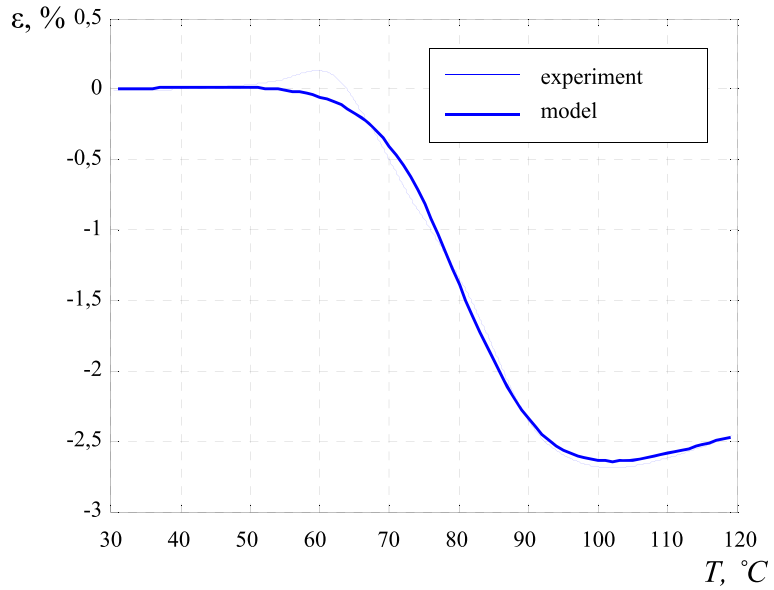

Fig. 2 Thermomechanical curve of epoxy specimen: experimental and numerical results

numerical results by minimizing the functional discrepancy. It was established numerically that the variation of γL and T_g does not affect the thermomechanical curve beyond the transition region. Therefore, the minimization parameters in this case were α_1, α_2 and E_1 with the normalizing factors 10^5, 10^5 and 10^{-4} respectively. The experimental and numerical deformation values were linearly interpolated to the temperature grid nodes with the 1°C increment. Then the value of functional discrepancy for temperatures beyond the transition region was calculated as a mean square discrepancy between the experimental and numerical data:

$$\psi = \sqrt{\frac{\sum_{i=1}^{n} \Delta\varepsilon_i{}^2}{n}}, \quad (5)$$

where n is the node number and $\Delta\varepsilon_i$ —the difference between the experimental and theoretical deformation values in the i node. For the functional minimization we use the quasi-Newton method of linear search. The iteration process stops when the current increment of the minimization parameter becomes less than 10^{-6}.

When the values of α_1, α_2 and E_1 are defined, we find T_g and γL by minimizing the functional discrepancy (5) within the transition temperature region. We use the same quasi-Newton method; for the parameter T_g the normalizing factor 0.1 was introduced.

From the functional minimization the following values of the model parameters were found: $\alpha_1 = 15.77 * 10^{-5}$, $\alpha_2 = 1.69 * 10^{-5}$, $E_1 = 296.76$ kPa, $T_g = 36.62$ ° C, and $\gamma L = 6.17$ ° C, which correspond to the mean square discrepancy of $7.17*10^{-4}$. The resultant approximation of experimental data with the numerical model is shown in Fig. 2.

Bending of axially compressed polymeric rod under temperature change. Problem formulation

In this section, the thermomechanical behavior of a rod with the spherical joint bonds on the boundaries is discussed. The rod is axially compressed with the force P that exceeds the critical one, which leads to buckling and subsequent bending (Fig. 3).

The loading path is the following (Fig. 4):

1) Loading with the force P at an initial temperature greater than $T_{g2}(N = 0)$;
2) Cooling under a constant load to a temperature less than T_{g1};
3) Unloading ($N = 1$); and
4) Heating to the initial temperature.

For a bended beam, the following expression is suitable (Rabotnov 1988):

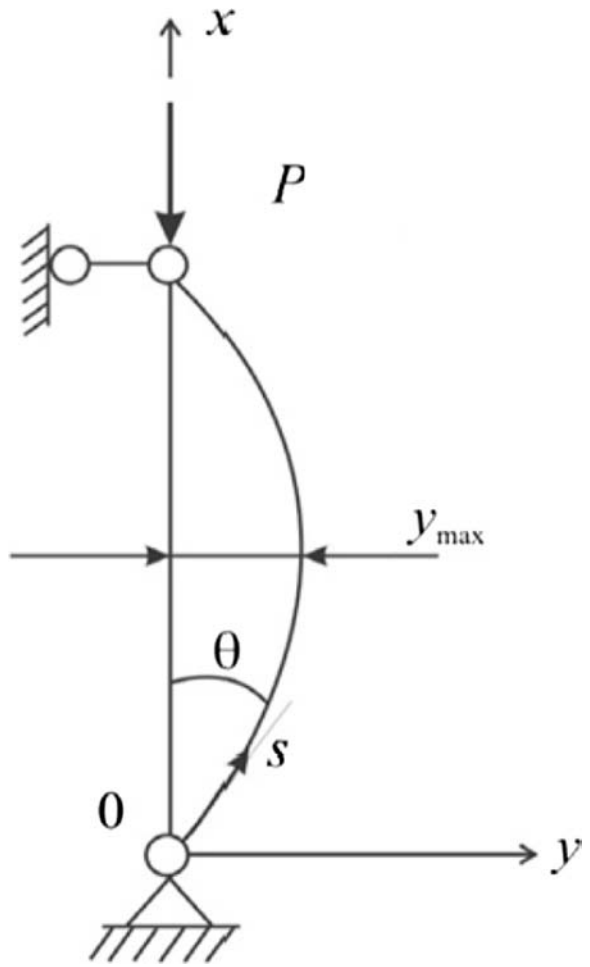

Fig. 3 Schematic representation of the compressed rod

$$\chi = \frac{M}{EI},$$

where $M = Py$ is the bending moment, y —the transverse coordinate (Fig. 3), I —the second moment of area, χ —the curvature. Then the constitutive equations (1) could be written as

$$\frac{P(t)\cdot y(t,s)}{I} = E_1\chi(t,s) + E_2\int_0^t (\chi(t,s) - \chi^*(\tau,s))dN(T(\tau)), \quad (6)$$

where s is the curvilinear axial coordinate with the zero point lying on the rod boundary, χ^* —the curvature at $t = \tau^*$; τ^* is the same as in (1). Here we do not consider the temperature expansion.

Thus, the mathematical statement of the problem includes the following relations:

- Constitutive equations (6);

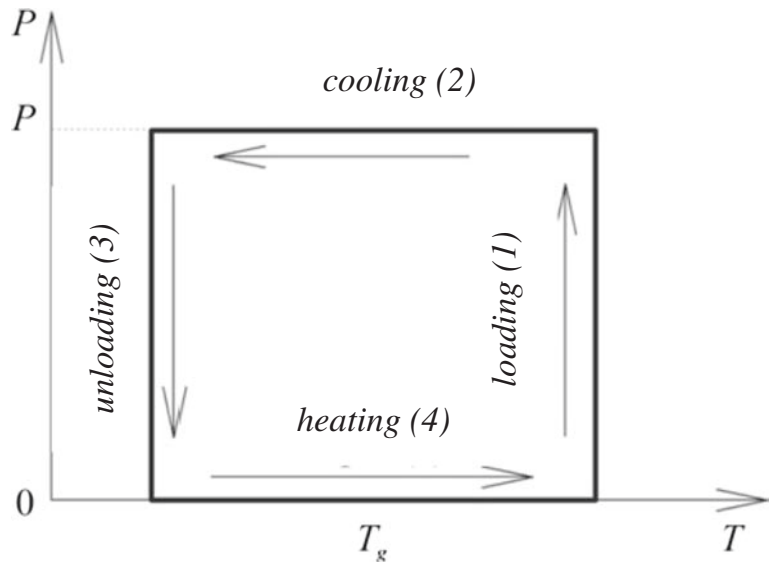

Fig. 4 A loading path

- Geometrical relations:

$$\chi = \frac{\partial \Theta}{\partial s}, \tag{7}$$

where Θ is the slope of the tangent line to the rod axis (Fig. 3); and

- Boundary conditions:

– zero boundary curvature: $\frac{\partial \Theta}{\partial s}\big|_{s=0} = 0$;
– a symmetry condition: $\Theta|_{s=l/2} = 0$.

Initially, the rod was in the rubbery material state, unloaded and undeformed: $P = 0, \chi = 0, N = 0$. At the first stage of the loading path (Fig. 4), the rod was loaded at a constant temperature. Considering that $\frac{\partial \gamma}{\partial s} = \sin\Theta$, the mathematical statement for this stage could be rewritten in the second-order differential form for the variable $\Theta(s)$ with boundary conditions:

$$\begin{cases} \dfrac{\partial^2 \Theta}{\partial s^2} = -\dfrac{P}{E_1 I}\sin\Theta \\ \dfrac{\partial \Theta}{\partial s}\Big|_{s=0} = 0 \\ \Theta\Big|_{s=l/2} = 0 \end{cases}. \tag{8}$$

In (Rabotnov 1988) the analytical solution of the Euler's elastica system (8) is given. The following equivalent variables are introduced:

$$\sin\frac{\Theta}{2} = m \cdot \sin\phi, \tag{9}$$

where $m = \sin\frac{\Theta_0}{2}$, $\Theta_0 = \Theta|_{s=0}$, and ϕ changes from 0 ($s = l/2$) to $\pi/2$($s = 0$). As a result, (8) is transformed to:

$$s = \sqrt{\frac{E_1 I}{P}} \cdot (F - F(\phi)), \tag{10}$$

where $F = \int_0^{\pi/2} \frac{d\phi}{\sqrt{1 - m^2 \sin^2\phi}}$ and $F(\phi) = \int_0^{\phi} \frac{d\phi}{\sqrt{1 - m^2 \sin^2\phi}}$ are the first type elliptic integrals. Upon substituting the boundary condition $\phi|_{s=l/2} = 0$ into (10) we obtain $F = \sqrt{\frac{P}{E_1 I}} \cdot \frac{l}{2}$, from which the value m for every particular load P could be unambiguously found. Then we can straightforwardly move from the relations $\Theta(\phi)$ (9) and $s(\phi)$ (10) to the relation $\Theta(s)$, and find the curvature $\chi_1(s)$ for the first loading stage from the geometrical equations (7).

During the loading stage 2 the load remains unchanged. According to the accepted hypotheses, every additional bond formed during vitrification is undeformed at its initiation moment, and so it does not affect the stress-strain state of the construction at that moment (Matveenko et al. 2012). Therefore, the curvature during cooling under a constant load remains unchanged: $\chi_2(s) = \chi_1(s)$.

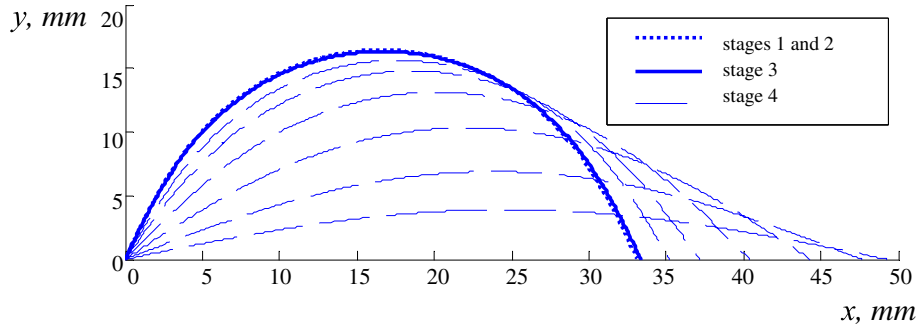

Fig. 5 Deformed rod shapes during different loading stages

Taking into consideration the absence of load at stages 3 and 4 and constancy of the curvature χ^* frozen during stage 2, the relations (6) could be rewritten as

$$0 = (E_1 + E_2 N(t))\chi(t,s) - \chi_2(t,s)E_2 \int_0^t dN(T(\tau)). \tag{11}$$

Thus, at stage 3, after unloading, with $N = 1$ the curvature is $\chi_3(t,s) = \frac{E_2}{E_1+E_2}\chi_2(t,s)$. The value $\frac{E_2}{E_1+E_2} < 1$, which corresponds to the curvature decrease after unloading.

During heating of the unloaded rod (stage 4) its curvature is defined as $\chi_4(t,s) = \frac{E_2 N(T(t))}{E_1+E_2 N(T(t))}\chi_2(t,s)$, which follows from (11). At the final temperature, the conversion degree parameter $N = 0$, therefore $\chi = 0$, i.e. the rod is fully straightened.

Results and discussion

In this section, we specify the problem formulated in the previous section for the 50 mm epoxy resin rod with a circular cross-section of 5 mm diameter. The material characteristics were found from the experiments described above.

It has been established from compressing tests for the rubbery material under different loads that for the deformations to be fully recoverable the stress should be less than 58 kPa. During bending of an axially compressed rod of the considered shape the respective load is 0.0435 N, which exceeds the critical one (Rabotnov 1988) 1.21 times. This value was taken as a compressing load P for our numerical simulations. The obtained results are demonstrated in Figs. 5 and 6.

As one can see in Figs. 5 and 6, maximum deflection corresponds to the first loading step at the rubbery material state, because the elastic modulus is very low at this temperature. The road being linear under a load less than the critical one causes the break of the curve (Fig. 6,

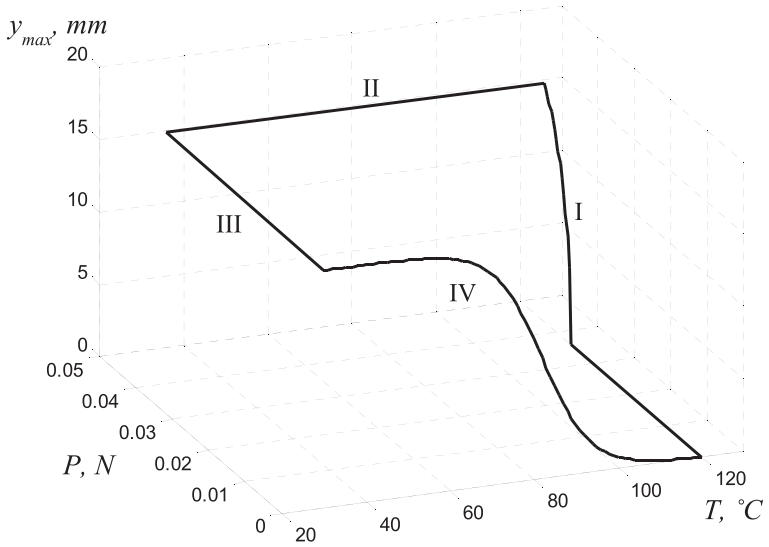

Fig. 6 Maximum deflection as a function of load and temperature during different loading stages

stage 1). The increase in load leads to buckling and a further nonlinear increase in deflection.

At the second stage—cooling under a constant load—the deformation remains constant. Here, according to the accepted hypotheses, the additional bond formation occurs, and every new bond is undeformed at its initiation moment. Therefore, the rigidity increase does not lead to additional strains and stresses.

At the third stage, after unloading the deflection decreases by a small value of about 0.8 % compared to the one at the first stage, because the elastic modulus at this temperature significantly exceeds the initial one. During subsequent heating (stage 4) the rod progressively straightens because of the molecular mobility growth, and the deformations frozen at stage 2 release.

Conclusions

In this research, we have studied the thermomechanical behavior of an axially compressed epoxy rod in its post-buckled equilibrium state. The thermomechanical shape-memory cycle has been modeled, which includes the stages of deformation development and preservation and the subsequent recovery of the initial shape. The material parameters included in constitutive equations were found from thermomechanical experiments. As a result, the deformed shapes of the rod in its post-buckled equilibrium state under changing temperature conditions have been obtained, and the shape memory effect has been illustrated.

Competing interests

The authors declare that they have no competing interests.

Authors' contribution

KT carried out this study and drafted the manuscript. NT supervised the research, planned the study, contributed to the interpretation of results and writing of the manuscript. All the authors read and approved the manuscript.

Acknowledgements

This work was supported by the Russian Foundation for Basic Research (project number 13-01-00553a).
We are especially grateful to prof. IN Shardakov of ICMM UB RAS and lead engineer SN Lysenko of ITC UB RAS for supplying materials and experimental support.

Author details

[1]Laboratory of Nonlinear Mechanics of Solids, Institute of Continuous Media Mechanics, Academician Korolev Street, Perm 614013, Russia. [2]Department of Computational Mathematics and Mechanics, Perm National Research Polytechnic University, Komsomolsky prospekt, Perm 614990, Russia.

Received: 10 September 2015 Accepted: 13 January 2016

References

Bartenev GM, Barteneva AG (1992) Relaxation Properties of Polymers. Chemistry, Moscow
Bolotin VV (1972) To the theory of viscous elasticity for structurally unstable operators. Works of MEI Dyn. Strength Mach 101:7–14
Bronshtein IN, Semendjaiev KA (1986) Mathematics Reference Book for Engineers and Students of Technical Institutes. Nauka, Moscow
Bugakov II (1989) Constitutive equations for materials with phase transition. J Mech Solids 3:111–117
Hager MD, Bodea S, Weber C, Schubert US (2015) Shape memory polymers: past, present and future developments. Prog Polym Sci 49–50:3–33. doi:10.1016/j.progpolymsci.2015.04.002
Il'ushin AA, Pobedria BE (1970) Fundamentals of the mathematical theory of thermoviscous elasticity. Nauka, Moscow
Klychnikov LV, Davtjan SP, Khudjaiev SI, Enikolopjan NS (1980) On the effect of inhomogeneous temperature field on the distribution of residual stresses under frontal solidification conditions. J Mech Compos Mater 13:509–513
Krylov AN (1931) About equilibrium forms of compressed columns under longitudinal bending. Izvestija Akademii nauk SSSR. VII series. Otdelenie matematicheskih i estestvennyh nauk 7:963–1012
Liu H, Uhlherr A, Bannister MK (2004) Quantitative structure–property relationships for composites: prediction of glass transition temperatures for epoxy resins. Polymer 45(6):2051–2060. doi:10.1016/j.polymer.2004.01.008
Matveenko VP, Smetannikov OY, Trufanov NA, Shardakov IN (2012) Models of thermomechanical behavior of polymeric materials undergoing glass transition. J Acta Mech 223:1261–1284. doi:10.1007/s00707-012-0626-z
Michels J, Widmann R, Czaderski C, Allahvirdizadeh R, Motavalli M (2015) Glass transition evaluation of commercially available epoxy resins used for civil engineering applications. J Composites Part B Eng 77:484–493. doi:10.1016/j.compositesb.2015.03.053
Moskvitin VV (1972) The strength of viscoelastic materials as applied to solid propellant charges of rocket engines. Nauka, Moscow
Rabotnov YN (1988) Mechanics of deformed solid body. Nauka, Moscow
Shardakov IN, Trufanov NA, Begishev VP, Shadrin OA (1991) Description of hereditary effects during vitrification and softening of epoxy resins. J Plasticheskie massy 9:55–58
Sharifi S, van Kooten TG, Kranenburg H-JC, Meij BP, Behl M, Lendlein A, Grijpma DW (2013) An annulus fibrosus closure device based on a biodegradable shape-memory polymer network. J Biomaterials 34:8105–8113. doi:10.1016/j.biomaterials.2013.07.061
Vol'mir AS (1967) Stability of deformed systems. Nauka, Moscow
Yakacki CM, Gall K (2010) Shape-memory polymers for biomedical applications. In: Lendlein A (ed) Shape-memory polymers. Springer Berlin Heidelberg, Berlin
Yakacki CM, Shandas R, Lanning C, Rech B, Eckstein A, Gall K (2007) Unconstrained recovery characterization of shape-memory polymer networks for cardiovascular applications. J Biomaterials 28:2255–2263. doi:10.1016/j.biomaterials.2007.01.030